JACS
JOURNAL OF THE AMERICAN CHEMICAL SOCIETY
Article
Cite This: J. Am. Chem. Soc. XXXX, XXX, XXX−XXX
pubs.acs.org/JACS

Solvent Tunes the Selectivity of Hydrogenation Reaction over α-MoC Catalyst

Yuchen Deng,[†,#] Rui Gao,[§,∥,⊥,#] Lili Lin,[†,#] Tong Liu,[†] Xiao-Dong Wen,[§,∥] Shuai Wang,[*,‡] and Ding Ma[*,†]

[†]Beijing National Laboratory for Molecular Sciences, College of Chemistry and Molecular Engineering and College of Engineering, and BIC-ESAT, Peking University, Beijing 100871, P. R. China

[‡]State Key Laboratory for Physical Chemistry of Solid Surfaces, Collaborative Innovation Center of Chemistry for Energy Materials, and National Engineering Laboratory for Green Chemical Productions of Alcohols-Ethers-Esters, College of Chemistry and Chemical Engineering, Xiamen University, Xiamen 361005, China

[§]State Key Laboratory of Coal Conversion, Institute of Coal Chemistry, Chinese Academy of Sciences, Taiyuan, 030001, China

[∥]National Energy Center for Coal to Liquids, Synfuels China Company, Ltd., Beijing 101400, China

[⊥]School of Chemistry and Chemical Engineering, Inner Mongolia University, Hohhot 010021, China

Supporting Information

ABSTRACT: Selective activation of chemical bonds in multifunctional oxygenates on solid catalysts is a crucial challenge for sustainable biomass upgrading. Molybdenum carbides and nitrides preferentially activate C═O and C−OH bonds over C═C and C−C bonds in liquid-phase hydrogenation of bioderived furfural, leading to highly selective formations of furfuryl alcohol (FA) and its subsequent hydrogenolysis product (2-methyl furan (2-MF)). We demonstrate that pure-phase α-MoC is more active than β-Mo_2C and γ-Mo_2N for catalyzing furfural hydrogenation, and the hydrogenation selectivity on these catalysts can be conveniently manipulated by alcohol solvents without significant changes in reaction rates (e.g., > 90% yields of FA in methanol solvent and of 2-MF in 2-butanol solvent at 423 K). Combined experimental and theoretical assessments of these solvent effects unveil that it is the hydrogen donating ability of the solvents that governs the hydrogenation rate of the reactants, while strong dissociative adsorption of the alcohol solvent on Mo-based catalysts results in surface decoration which controls the reaction selectivity via enforcing steric hindrance on the formation of relevant transient states. Such solvent-induced surface modification of Mo-based catalysts provides a compelling strategy for highly selective hydrodeoxygenation processes of biomass feedstocks.

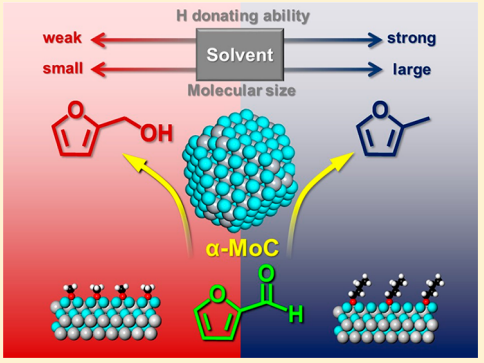

1. INTRODUCTION

Furfural is widely identified as a key platform molecule for catalytic upgrading of biomass-derived feedstocks into useful fuels and chemicals because of its multifunctional characteristic, consisting of carbonyl (C═O) and π-conjugated (C═C−C═C) groups and a five-membered ring structure, and also based on the fact that it has already been manufactured from C_5 sugars in a commercial scale (over 280 000 ton per year).[1] In particular, selective conversions of furfural to furfuryl alcohol (via hydrogenation) and to 2-methyl furan (via secondary hydrogenolysis of furfuryl alcohol, Scheme 1) are highly desired. Both of these products are essential raw materials for chemical industry. For instance, furfuryl alcohol is the starting material for the synthesis of furan resins,[2] whereas 2-methyl furan has a high blending research octane number (RON) of 103 and low water solubility, making itself a promising fuel additive for gasoline.[3]

The synthesis of furfuryl alcohol and 2-methyl furan from furfural are more preferable to be conducted in liquid phase than in gas phase, in view of high energy consumption for vaporizing furfural reactants in the latter case.[4] The core challenges in these cascaded syntheses are (1) to avoid side reactions, such as dimerization of furfural to C_{10} species (and subsequent hydrogenation and dehydration reactions), decarbonylation of furfural to furan, and C═C bond hydrogenation and ring opening reactions for furfural, furfuryl alcohol and 2-methyl furan (Scheme 1),[5] and (2) to control the hydrogenation/hydrogenolysis extent to obtain either furfuryl alcohol or 2-methyl furan exclusively.[6] To overcome the first hurdle, various supported metal catalysts (e.g., Pd,[7−9] Pt,[10−13] Ru,[14−17] Fe,[4] Cu,[6,18−21] Ni,[22−24] and Co[25]) and molybdenum carbides (e.g., β-Mo_2C[26,27]) have been studied for furfural hydrogenation in liquid media. Among these solid catalysts, Cu and molybdenum carbide show superior selectivities to furfuryl alcohol and 2-methyl furan, reflecting

Received: August 31, 2018
Published: October 15, 2018

DOI: 10.1021/jacs.8b09310
J. Am. Chem. Soc. XXXX, XXX, XXX−XXX

Scheme 1. Reaction Pathways for Hydrogenation of Furfural to Furfuryl Alcohol and 2-Methyl Furan (Solid Arrows) and Plausible Side Reactions of the Reactants and Products (Dashed Arrows)

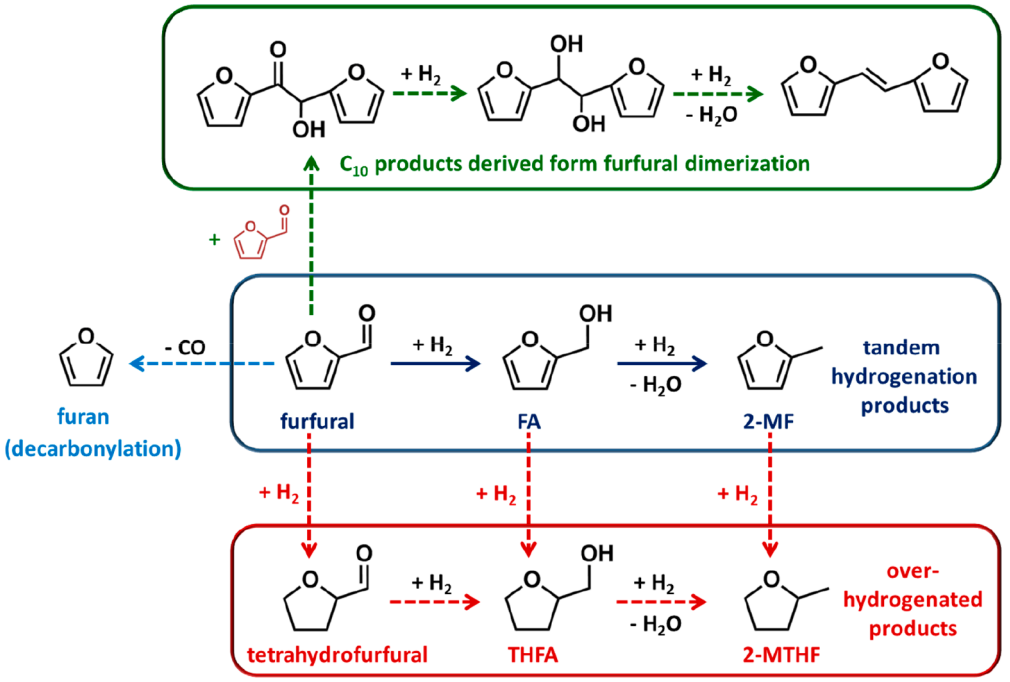

their preferential activation of C═O and C−OH bonds over C═C and C−C bonds. Alternatively, the relative selectivities between furfuryl alcohol and 2-methyl furan are commonly altered by reaction temperature. For instance, high yields of furfuryl alcohol (>80%) were achieved on Cu/SiO_2 catalysts at 413 K, while such high yields of 2-methyl furan on the same Cu catalysts required an increase of the reaction temperature up to 473 K.[6] This temperature strategy, however, requires high energy spent in accelerating hydrogenolysis of the primary furfuryl alcohol products to obtain high 2-methyl furan selectivities, rendering it impractical for controlling the selectivity of furfural hydrogenation at mild reaction conditions.

Modification of solid catalyst surfaces by organic species provides another means to mediate reaction rates and selectivities via changing the electronic property or steric environment of active sites.[8,28,29] Transition metal carbides have shown similar or even better catalytic activities than noble metals in certain types of hydrogenolysis reactions,[30] and the strong dissociative adsorption of alcohols on molybdenum carbides[31,32] inspires us that the use of alcohol solvents for furfural hydrogenation reactions on molybdenum carbide catalysts would make those molybdenum carbide surfaces decorated by alcohol-derived species in situ. Moreover, several reports have shown alcohol solvents can act as hydrogen donors to improve hydrogenation and hydrogenolysis rates.[33] We thus expect that alcohol solvents would strongly influence both furfural hydrogenation rates and selectivities on molybdenum carbide catalysts. It is also worth noting that only β-Mo_2C among the known molybdenum carbide crystalline phases has been examined in furfural hydrogenation reactions.[27,34] Our recent results, however, show that α-MoC exhibits higher oxophilicity than β-Mo_2C,[31,35] indicating the former crystalline phase is catalytically more active for hydrodeoxygenation.

In this work, we report that pure-phase molybdenum carbides (α-MoC, β-Mo_2C) and nitrides (γ-Mo_2N) selectively catalyze liquid-phase hydrogenation of furfural to furfuryl alcohol and 2-methyl furan at low temperatures, in which α-MoC shows both higher activity and 2-methyl furan selectivity than the other Mo-based catalysts. Effects of solvents (C_1−C_4 alcohols, cyclohexane, and H_2O) for furfural hydrogenation on α-MoC are rigorously assessed here via combined experimental and theoretical methods. We demonstrate that alcohol solvents are preferred for selective hydrogenation of furfural, because their hydrogen donating ability promotes hydrogenation rates, and their dissociative adsorption on α-MoC leads to alkoxide-decorated catalyst surfaces that render the selectivities of furfuryl alcohol and 2-methyl furan controllable from end to end via changing the size of alcohol solvent molecules even at similar furfural hydrogenation rates. This in situ modification of molybdenum carbide catalysts by functional alcohol solvents provides a convenient strategy to mediate reactivity and selectivity of liquid-phase hydrodeoxygenation processes, which appears to be versatile for upgrading biomass-derived oxygenates.

2. EXPERIMENTAL SECTION

2.1. Catalyst Preparation. Synthesis details of Mo-based catalysts have been reported previously,[31] and thus only a brief description is provided here. MoO_3 was prepared first via calcination of $(NH_4)_2Mo_7O_{24}{\cdot}4H_2O$ (>99.0%, Sinopharm Chemical) in stagnant air at 773 K for 4 h. These MoO_3 powders were heated to 973 K (10 K min^{-1}) in flowing NH_3 (160 mL min^{-1}; prepurified gas) and held at 973 K for 2 h, and then treated in flowing 20% CH_4/H_2 (125 mL min^{-1}; prepurified gas) at the same temperature for 2 h to obtain pure-phase α-MoC. β-Mo_2C was prepared by heating MoO_3 powders to 973 K (from ambient temperature to 573 at 5 K min^{-1} and from 573 to 973 at 1 K min^{-1}) in flowing 20% CH_4/H_2 (125 mL min^{-1}) and held at 973 K for 2 h. γ-Mo_2N was prepared similarly by treating MoO_3 powders in flowing NH_3 (160 mL min^{-1}; prepurified gas) at 973 K (10 K min^{-1}) for 2 h. Two wt % Ni/SiO_2, used here as a

DOI: 10.1021/jacs.8b09310
J. Am. Chem. Soc. XXXX, XXX, XXX−XXX

Table 1. Conversion and Selectivities of Liquid-Phase Furfural Hydrogenation on Mo-Based Solid Catalysts and Ni/SiO_2[a]

entry	catalyst	H_2 pressure (MPa)	furfural conversion (%)	product selectivity[b] (%)				
				2-MF	FA	2-MTHF	THFA	others
1	α-MoC	1	72.2	48.4	25.1	0	0	26.5
2	α-MoC	2	96.5	81.8	5.9	0	0	12.3
3	α-MoC	3	96.6	89.8	10.2	0	0	0
4	β-Mo_2C	2	66.9	48.9	38.9	0	0	12.2
5	γ-Mo_2N	2	21.0	5.6	61.8	0	1.0	31.6
6	α-MoC (passivated)	2	74.3	66.8	33.2	0	0	0
7	MoO_2	2	1.0	0.1	0.9	0	0	99.0
8	MoO_3	2	1.1	0.1	1.0	0	0	98.9
9	Ni/SiO_2	3	>99.9	10.9	0.8	81.5	4.7	2.1

[a]Reaction condition: 150 mg catalyst, 1 mL furfural, 50 mL 2-propanol solvent, 423 K, 6 h. [b]2-Methyl furan (2-MF), furfuryl alcohol (FA), 2-methyl tetrahydrofuran (2-MTHF), tetrahydrofurfuryl alcohol (THFA), other products mainly including C_{10} species formed form dimerization of furfural and subsequent dehydration and hydrogenation reactions (Scheme 1).

reference hydrogenation catalyst, was synthesized using incipient wetness impregnation of commercial SiO_2 supports with $Ni(NO_3)_2$ aqueous solution, followed by drying at 393 K for 3 h, calcination in stagnant air at 773 K for 4 h, and reduction in flowing H_2 at 573 K (10 K min^{-1}) for 2 h.[36] All catalysts were passivated in flowing 0.5% O_2/Ar (55 mL min^{-1}) at ambient temperature for 12 h before exposure to air.

2.2. Catalyst Characterization. *2.2.1. X-ray Diffraction (XRD).* XRD measurements were used to examine the identity and phase purity of the synthesized catalysts (Cu Kα radiation, λ = 0.15418 nm, 40 kV, 40 mA; 2θ: 20°−80°, 8° min^{-1}; PANalytical X'Pert).

2.2.2. X-ray Absorption Fine Structure (XAFS) Spectroscopy. XAFS spectra were measured in transmission mode at the Mo−K-edge (20,000 eV) using the BL14W beamline of the Shanghai Synchrotron Radiation Facility and an ion chamber as the detector. Mo foil, MoO_2 (Aldrich) and MoO_3 (Aldrich) were used as references. Before measurement, α-MoC and β-Mo_2C were pretreated in a mixture of 15% CH_4/H_2 (40 mL min^{-1}) at 863 K for 2 h, whereas γ-Mo_2N was pretreated in a NH_3 flow (40 mL min^{-1}) at the same temperature for 2 h. These samples were then carefully sealed under argon protection in a glovebox. All XAFS spectra were analyzed using the Ifeffit package.[37] A backscattering equation with FEFF models[37] generated from known crystal structures (space group: Fm3m for α-MoC, P63/mmc for β-Mo_2C) was used for the fitting of the extended XAFS oscillation.

2.2.3. X-ray Photoelectron Spectroscopy (XPS). The chemical state of Mo-atoms exposed on α-MoC, β-Mo_2C, and γ-Mo_2N catalysts was determined using an Axis ultraimaging photoelectron spectrometer (Kratos Analytical). These samples were activated in a quartz tube by flowing gas (15% CH_4/H_2 for α-MoC and β-Mo_2C; NH_3 for γ-Mo_2N; 40 mL min^{-1}) at 863 K for 2 h, and were then transferred into the chamber of the XPS spectrometer under argon protection for measurements.

2.2.4. Electron Microscopy. Scanning/transmission electron microscopy (S/TEM) characterizations were conducted using FEI Talos F200X equipped with Super-X EDX operating at 200 kV. All samples were dispersed in ethanol by ultrasonication. The suspension was then deposited onto a copper grid with carbon film for measurements.

2.3. Furfural Hydrogenation Reactions. Furfural hydrogenation reactions were carried out in a 150 mL stainless-steel autoclave. One mL furfural (>99%, Sinopharm Chemical) and 50 mL organic solvent (methanol and ethanol, > 99.7%, Xilong Scientific; 2-propanol and *tert*-butanol, >99.5%, Beijing Tongguang; 2-butanol, >99%, Sinopharm Chemical) previously deaerated by argon flow for 15 min, together with a certain amount of Mo-based catalysts (0−300 mg), were loaded into the autoclave. The autoclave was sealed and purged by H_2 (>99.999%, Beijing Nanfei) three times, pressurized with H_2 to the desired values (1−3 MPa), and then heated to the reaction temperature (stirring speed at 800 rpm to ensure the removal of mass transfer effects during catalysis; Figure S1 in Supporting Information, SI). The concentrations of furfural and reaction products were analyzed using gas chromatograph (Agilent 7820A) equipped with a flame ionization detector and a Agilent HP-INNOWWax column (30 m, 0.32 mm ID; 0.25 μm film), in which decahydronaphthalene (>99.5%, Sinopharm Chemical) was used as an external calibration agent for quantifying furfural conversions and product selectivities. The chemical identity of the products was confirmed by a mass selective detector (Agilent 5975) after separation by gas chromatograph (Agilent 7820A) equipped with a nonpolar HP-5MS column (30 m, 0.25 mm ID; 0.25 mm film). The carbon balance was typically above 95%, and the product selectivities were reported here on a carbon basis.

2.4. Density Functional Theory Methods. All calculations were carried out using periodic plane-wave density functional theory (DFT) methods as implemented in the Vienna ab initio simulation package (VASP).[38,39] The interaction between electrons and ion cores was described with the projector augmented wave (PAW) method (energy cutoff 450 eV),[40,41] whereas the electronic exchange and correlation energies were described using the Perdew−Burke−Ernzerhof (PBE) functional under the generalized gradient approximation.[42] Electron smearing was treated by the Methfessel−Paxton technique[43] with a constant smearing width of 0.2 eV. Spin polarization and van der Waals interaction among atoms (calculated via Grimme's DFT-D3 method with Becke-Jonson damping[44]) were both taken into account during each geometric optimization step, and the climbing image nudged elastic band method (CI-NEB)[45] was used to determine transition state structures. Vibrational frequency analyses were performed to examine optimized structures (no imaginary frequency for a steady state; a single imaginary frequency for a transition state).

The α-MoC (111) surface slabs were built from DFT-derived pure-phase α-MoC structures (face center cubic, lattice constant 0.4332 nm) as described elsewhere.[31] These slabs have been shown to represent adequate models for simulating catalytic reactions on α-MoC.[31,35] Specifically, a p(4 × 4) α-MoC(111) supercell with three Mo-atom layers and three C-atom layers overlaid alternatively (16 atoms per layer; Figure S2 in the SI) were used to assess the elementary steps involved in furfural hydrogenation on α-MoC. During these simulations, the atoms in the bottom three layers of the α-MoC (111) supercell were fixed, while the other atoms were allowed to move freely. A 3 × 3 × 1 Monkhorst-pack[46] sampling of the first Brillouin zone (k-point mesh) was applied to obtain accurate electronic energy.

3. RESULTS AND DISCUSSION

3.1. Activity and Selectivity of Liquid-Phase Furfural Hydrogenation Reactions on Mo-based Catalysts. Pure-phase α-MoC, β-Mo_2C, and γ-Mo_2N catalysts were prepared from MoO_3 through different reducing treatments as reported previously.[31] The purity of their crystalline phases was

DOI: 10.1021/jacs.8b09310
J. Am. Chem. Soc. XXXX, XXX, XXX−XXX

confirmed by X-ray diffraction (XRD) measurements (Figures S3 and S4 in the SI). For instance, the XRD pattern of the synthesized α-MoC catalyst exhibited exclusive peaks at 37.0°, 42.6°, 62.4°, and 74.4° within the 2θ range of 20°−80°, consistent with those predicted theoretically.[31] Transmission electron microscopy (TEM) characterization showed that these catalysts had porous appearance with highly textured nanocrystals of 2−10 nm in size (Figures S5−S7). The activity and selectivity of liquid-phase furfural hydrogenation reactions on these Mo-based catalysts were examined at 423 K and 1−3 MPa H_2. 2-Propanol and 2-butanol were used as solvent in these experiments, because they are capable of donating hydrogen to promote rates of such hydrogenation reactions.[14]

Table 1 shows that furfural hydrogenation reactions took place on α-MoC with high selectivities to 2-methyl furan (2-MF) and furfuryl alcohol (FA), and no products derived from hydrogenation of the C═C bonds in furfural (e.g., tetrahydrofurfuryl alcohol (THFA) and 2-methyl tetrahydrofuran (2-MTHF); the pathway with red dashed lines, Scheme 1) were observed, indicative of preferential activation of C═O and C−OH bonds over C═C bonds on α-MoC surfaces. For instance, the selectivities of 2-methyl furan and furfuryl alcohol were 48.4% and 25.1%, respectively, at 72.7% furfural conversion (423 K, 1 MPa H_2; Entry 1, Table 1), whereas side products with a total selectivity of 26.5% were mainly C_{10} species that were formed from competitive dimerization of furfural and subsequent dehydration and hydrogenation reactions (the pathway with green dashed lines, Scheme 1). These side reactions were gradually restrained as the H_2 pressure increased (Entries 2 and 3, Table 1), because of faster scavenging of furfural through the hydrogenation reaction channel at higher H_2 pressures. As shown in Entry 3 of Table1, furfural converted to 2-methyl furan and furfuryl alcohol nearly exclusively at 3 MPa H_2 with their selectivities of 89.8% and 10.2%, respectively (at 96.6% furfural conversion).

The increase of H_2 pressure from 1 to 3 MPa led to an increase of the 2-methyl furan selectivity from 48.4% to 89.8% and a concomitant decrease of the furfuryl alcohol selectivity from 25.1% to 10.2% (Entries 1 and 3, Table 1). These changes indicate that 2-methyl furan is formed from hydrogenolysis of furfuryl alcohol (the pathway with blue solid lines, Scheme 1) and thus a secondary product in furfural hydrogenation, agreed well with similar inverse changes of these selectivities as the furfural conversion increases (Figure 1). The direct use of furfuryl alcohol as the reactant showed exclusive formation of 2-methyl furan with conversion rates higher than those for furfural at the same reaction conditions (Table S1), which further supports the proposed reaction pathway for furfural hydrogenation on α-MoC. It is also worth noting that furfural hydrogenation on Ni/SiO_2 catalysts at the same reaction condition led to overhydrogenated 2-methyl tetrahydrofuran (2-MTHF) as the main product (81.5% selectivity, Entry 9, Table 1), reflecting, in turn, the requirement of appropriate hydrogenation function for selective conversions of furfural to 2-methyl furan and furfuryl alcohol.

Furfural hydrogenation reactions catalyzed by β-Mo_2C and γ-Mo_2N also showed negligible selectivities to hydrogenation of the C═C bonds in furfural (Entries 4 and 5, Table 1), indicating that the hydrogenation preference for C═O bonds over C═C bonds is general to Mo-based catalysts. Furfural conversions on β-Mo_2C (66.9%, Entry 4) and γ-Mo_2N (21.0%, Entry 5) obtained at 423 K and 2 MPa H_2, however, were

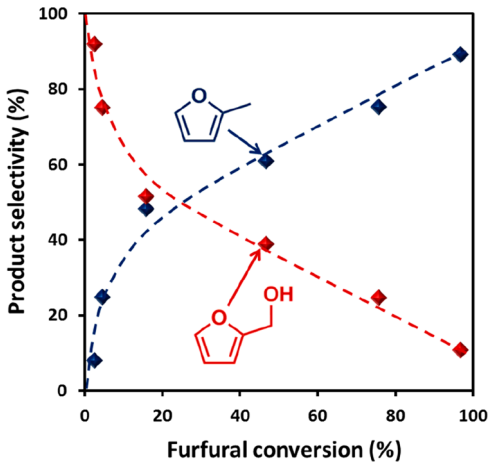

Figure 1. Selectivities of furfuryl alcohol and 2-methyl furan as a function of furfural conversion on α-MoC catalysts (423 K, 2.0 MPa H_2, 1 mL furfural, 50 mL 2-butanol solvent). Dashed curves indicate quantitative trends.

significantly lower than those on α-MoC (96.5%, Entry 2), in concomitance with much lower selectivities to 2-methyl furan on the former catalysts (β-Mo_2C 48.9%; γ-Mo_2N 5.6%; α-MoC 81.8%). It is thus suggested that the α-MoC phase is the most active and selective Mo-based structures for catalyzing furfural hydrogenation to 2-methyl furan. In particular, the Mo centers in α-MoC and β-Mo_2C phases have similar positive charges as measured from both X-ray photoelectron spectroscopy (XPS) and X-ray absorption near-edge structure (XANES) spectroscopy (Figures S8 and S9), while the extended X-ray-absorption fine-structure (EXAFS) analysis showed that such Mo centers in α-MoC had a higher average coordination number for Mo−C interactions than those in β-Mo_2C (2.7 ± 0.9 vs 2.2 ± 0.8, Figures S10−S12 and Table S2), indicative of coordinationally more-unsaturated Mo sites exposed on β-Mo_2C surfaces. Theoretical calculations shown in Section 3.3 suggest molybdenum carbides are fully covered by alcohol solvent molecules at catalytic conditions. Accordingly, we surmise that the alcohol solvent molecules are bound more strongly to β-Mo_2C than α-MoC, rendering the active sites on the former surfaces less accessible to the furfural reactants and thus lower furfural hydrogenation rates.

To further assess the chemical state of active sites exposed on α-MoC surfaces, α-MoC catalysts were passivated in flowing 0.5% O_2/Ar at room temperature for 12 h and then used for furfural hydrogenation reactions without further reductive activation. This passivation led to a decrease of the furfural conversion from 96.5% to 74.3% and also a decrease of the 2-methyl furan selectivity from 81.8% to 66.8% (Entry 6, Table 1). These changes indicate that MoO_x surface species derived from the passivation are inactive to catalyze furfural hydrogenation, consistent with the inert nature of MoO_2 and MoO_3 for such hydrogenation reactions (Entries 7 and 8, Table 1). However, it is worth addressing that the attack of molybdenum carbide surface by OH groups or O atoms coming from the alcohol solvent molecule or H_2O (present with a trace amount in the organic solvent or formed from hydrogenolysis of furfuryl alcohol) could slightly modify its surface during catalysis, and maybe it is more proper to describe the working surface as oxocarbide.[32]

The α-MoC catalysts deactivated gradually along with the process of furfural hydrogenation, despite their superior

DOI: 10.1021/jacs.8b09310
J. Am. Chem. Soc. XXXX, XXX, XXX−XXX

activity and selectivity to the activation of C═O and C−OH bonds. For instance, the conversion of furfural decreased form 98.4% to 20.5% after four consecutive runs at 423 K and 2.0 MPa H_2 (Figure S13a), concomitant with the 2-methyl furan selectivity decreased from 91.9% to 61.6% and the furfuryl alcohol selectivity increased from 8.1% to 38.9%. Such deactivation of metal carbides during catalysis is usually attributed to surface oxidation, coke formation, or structural change.[47] XRD characterization after reaction showed that the size and phase purity of the α-MoC catalysts were both well preserved at the examined reaction conditions (Figure S3). The contribution of surface oxidation to the deactivation also seems to be minor, because the decrease of activity caused by the oxidative passivation (22.2%; Entry 6, Table 1) is much less than the change in the four consecutive cycles (77.9%, Figure S13a). We thus propose that coke formation from the strongly bound unsaturated reaction intermediates on α-MoC surfaces accounts for the observed deactivation, in agreement with the retardation of deactivation by higher H_2 pressure during catalysis (Figure S13b). It is noted that metal carbides can often be effectively regenerated through hydrogen treatment after reaction,[47] which would make these materials practical for catalyzing hydrodeoxygenation of biomass feedstocks.

Taken together, pure-phase α-MoC catalysts present superior activity in hydrogenating the C═O bond of furfural to form furfuryl alcohol and 2-methyl furan, especially with a high selectivity to the latter in secondary alcohol solvents (e.g., 2-propanol and 2-butanol; further discussed below), at mild reaction conditions. Next, we show that solvent molecules are capable of mediating the selectivities of furfuryl alcohol and 2-methyl furan on α-MoC in an extremely wide range without a significant change of the furfural hydrogenation rates.

3.2. Solvent Effects on Activity and Selectivity of Furfural Hydrogenation on α-MoC Catalysts. Solvents are able to stabilize specific reaction intermediates or transition states bound to solid catalysts, thus resulting in strong dependence of reaction rates or selectivities on the polarity of solvents.[8,28,29] Moreover, solvents with hydrogen donating ability benefit hydrogenation reactions when hydrogenation rates are kinetically limited by steps involving H_2 activation.[14,44] These solvent effects for furfural hydrogenation on α-MoC catalysts are examined here with nonpolar cyclohexane and polar C_1−C_4 alcohols (i.e., ethanol, 1-propanol, 1-butanol, 2-propanol, 2-butanol, and *tert*-butanol). Among these solvent molecules, both of cyclohexane and *tert*-butanol lack hydrogen donating ability, whereas the others are good hydrogen donators.

Figure 2 shows that the yield of furfural hydrogenation products (i.e., the sum of furfuryl alcohol and 2-methyl furan) in cyclohexane (11.5%; corresponding to 1.6 $mmol_{furfural}\ g_{MoC}^{-1}\ h^{-1}$ in reaction rate, henceforth) was much lower than that in *tert*-butanol (39.4%; 5.6 $mmol_{furfural}\ g_{MoC}^{-1}\ h^{-1}$ in reaction rate) at 423 K and 2 MPa H_2, reflecting polar solvents favor furfural hydrogenation reactions because of the polar nature of the furfural reactants. For C_2−C_4 alcohol solvents, the yield of hydrogenation products increased as an order of tertiary alcohol (*tert*-butanol; 39.4%; 5.6 $mmol_{furfural}\ g_{MoC}^{-1}\ h^{-1}$ in reaction rate) < primary alcohol (ethanol, 1-propanol, and 1-butanol; 50.1%−65.5%; 7.2−9.4 $mmol_{furfural}\ g_{MoC}^{-1}\ h^{-1}$ in reaction rate) < secondary alcohol (2-propanol and 2-butanol; 84.7%−92.3%; 12.1−13.2 $mmol_{furfural}\ g_{MoC}^{-1}\ h^{-1}$ in reaction rate). This trend agrees well with their activity as a hydrogen donor in catalytic transfer hydrogenation reactions,[48] and thus indicates the involvement of primary/secondary alcohol solvents as a hydrogen source for promoting hydrogenation/hydrogenolysis rates on α-MoC surfaces. Similar effects of alcohol hydrogen donors on furfural hydrodeoxygenation rates have also been observed for supported metal catalysts (e.g., Fe[4] and Ru[16]). Such findings, in turn, provide evidence for the kinetically relevance of hydrogen transfer steps in furfural conversions on α-MoC surfaces, in line with the presence of primary kinetic isotope effects for furfural hydrogenation when H_2 is replaced by D_2 (k_H/k_D = 1.8 at 423 K; Table S3). Consistently, the yield of 2-methyl furan (derived from hydrogenolysis of the primary furfuryl alcohol products) was also much higher in the secondary alcohol solvents than those in the primary alcohol solvents (e.g., 90.6% vs 45.5% for 2-butanol and 1-butanol of similar sizes; 5.6 vs 13.0 $mmol_{furfural}\ g_{MoC}^{-1}\ h^{-1}$ in reaction rate), and their respective yields of furfuryl alcohol showed a revise order (1.7% for 2-butanol vs 20.0% for 1-butanol; 0.2 vs 2.9 $mmol_{furfural}\ g_{MoC}^{-1}\ h^{-1}$ in reaction rate). Similar promoting effects of alcohol hydrogen-donors on furfural hydrogenation were also observed on supported metal catalysts.[48] Isotopic labeling experiments[33] revealed that such catalytic transfer hydrogenation reactions follow the Lewis acid mediated Meerwein−Ponndorf−Verley (MPV) mechanism, in which the β-H atom of an alcohol is transferred to the carbonyl C atom of furfural via a concerted six-membered ring transition state on Lewis acid sites (shown in Scheme 2 using Mo sites exposed on the α-MoC surfaces as an illustrative example).

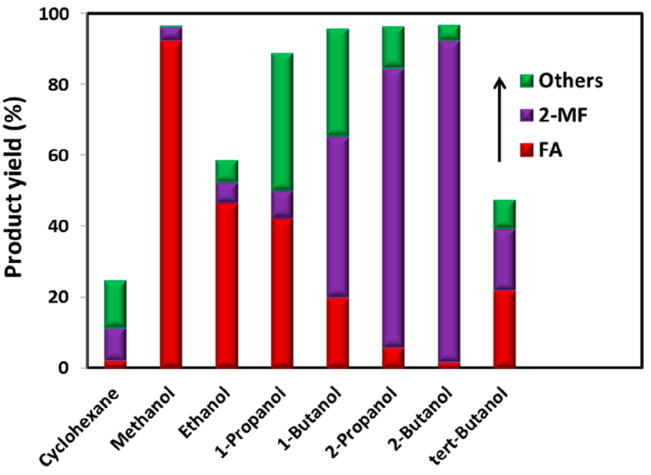

Figure 2. Solvent effects on product yields of furfural hydrogenation on α-MoC catalysts (423 K, 2.0 MPa H_2, 1 mL furfural, 50 mL solvent, 150 mg α-MoC, 6 h; FA for furfuryl alcohol, 2-MF for 2-methyl furan).

Negligible conversions of furfural on α-MoC were found in 2-butanol solvent when the H_2 atmosphere was replaced by N_2 (Table S3), suggesting H_2 is still the requisite for such catalytic transfer hydrogenation reactions on α-MoC. We surmise that the carbonyl compounds formed from the transfer hydrogenation of alcohol to furfural bind strongly to the α-MoC surface because of the high oxophilicity of metal carbides.[46] As a consequence, H_2 is required to scavenge these formed carbonyl compounds (via fast hydrogenation) in order to make α-MoC sites available for successive turnovers of furfural hydrogenation.

In contrast to the above solvent effects for C_2−C_4 alcohols, the yield of furfural hydrogenation products in methanol

DOI: 10.1021/jacs.8b09310
J. Am. Chem. Soc. XXXX, XXX, XXX−XXX

Scheme 2. Plausible Pathway for Transfer Hydrogenation of Furfural by an Alcohol on α-MoC Surfaces

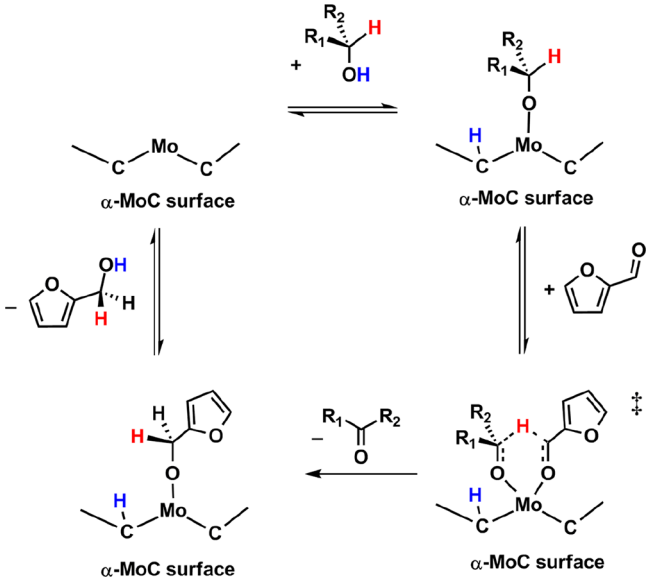

(96.2%, Figure 2; 13.8 $mmol_{furfural}\ g_{MoC}^{-1}\ h^{-1}$ in reaction rate) was much higher than those in the larger C_2−C_4 primary alcohol solvents (50.1%−65.5%; 7.2−9.4 $mmol_{furfural}\ g_{MoC}^{-1}\ h^{-1}$ in reaction rate) and similar to those in the secondary alcohol solvents (84.7%−92.3%; 12.1−13.2 $mmol_{furfural}\ g_{MoC}^{-1}\ h^{-1}$ in reaction rate). Moreover, the furfural hydrogenation in methanol exhibited an extremely high selectivity to furfuryl alcohol (>95% in the whole furfural conversion range, Figure S14), whereas the furfuryl alcohol selectivities ranged within 20.9%−79.1% for the C_2−C_4 primary alcohols and 1.8%−6.0% for the secondary alcohol solvents (Figure 2). Liquid-phase furfural hydrogenation on carbon-supported Fe catalysts, however, showed much lower rates and was much less selective to furfuryl alcohol in methanol than in 2-butanol.[4] As discussed in the next section, these distinct effects of methanol solvent for furfural hydrogenation on α-MoC (compared to Fe-based catalysts) are brought forth by the unique high coverage of alcohol-derived species on α-MoC surfaces during catalysis, which makes possible the convenient control of furfural hydrogenation selectivity via changing the size of alcohol solvent molecules even at similar furfural hydrogenation rates.

To sum up, the above data indicate that the selectivities of furfural hydrogenation to furfuryl alcohol and 2-methyl furan on α-MoC can be readily mediated from end to end using alcohol solvents with an appropriate size (e.g., methanol for furfuryl alcohol and 2-butanol for 2-methyl furan) without significant influence on furfural conversion rates. Theoretical calculations were used next to bring insights into these size effects of alcohol solvents at a molecular level.

3.3. Theoretical Assessment of the Size Effects of Alcohol Solvents for Furfural Hydrogenation on α-MoC Catalysts. Density function theory (DFT) treatments with α-MoC (111) surface models (Section 2.4) were applied here to elucidate the observed size effects of alcohol solvents on the rate and selectivity of furfural hydrogenation reactions on α-MoC. The α-MoC(111) surface is the predominant exposed surface of α-MoC as revealed from the high-resolution electron microscopy characterization.[31] Good correlations between experiments and theoretical treatments using α-MoC(111) surface models for water−gas shift[34] and aqueous-phase reforming of methanol[31] reactions further indicate that these α-MoC(111) surface models are adequate to examine physical and chemical processes occurred on α-MoC.

Dissociative adsorption energies for alcohols on α-MoC(111) surfaces to form bound alkoxide and H species (ΔE_{dis}) are defined here as the difference between the total energy for the separated alkoxide and H moieties bound to an α-MoC surface ($E_{RO^*+H^*}$) and the sum of energies for an alcohol molecule in gas phase ($E_{ROH(g)}$) and a bare α-MoC surface (E_{MoC}):

$$\Delta E_{dis} = E_{RO^*+H^*} - E_{ROH(g)} - E_{MoC} \quad (1)$$

Such ΔE_{dis} values reflect the intrinsic ability of alcohols to dissociate on α-MoC surfaces. DFT-derived ΔE_{dis} values for C_1−C_4 alcohols on α-MoC(111) surfaces were all quite negative (below −270 kJ mol^{-1}, Figure 3; DFT-optimized

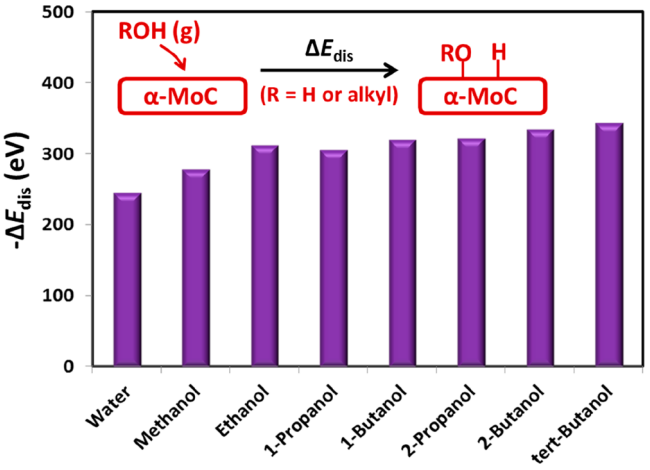

Figure 3. DFT-derived dissociative adsorption energies (ΔE_{dis}) for C_1−C_4 alcohols and H_2O on α-MoC(111) surfaces (with respect to gaseous state; surface coverage 0.06−0.11).

structures shown in Figure S15), indicating that the dissociation processes of these alcohol molecules are thermodynamically favored and thus rendering the α-MoC surfaces fully saturated by these solvent molecules during catalysis. It is worth noting that these ΔE_{dis} values were calculated at low coverages (defined as the ratio of the adsorbates to the exposed Mo sites on the α-MoC(111) surface; 0.06−0.11). The trend of the adsorption ability for the examined alcohols remains, however, at even saturation coverages (0.38−0.56; Figure S16). As a consequence, energy needs to be paid for desorbing alcohol solvent molecules from the covered α-MoC surfaces in order to make active sites available for furfural reactants.

The ΔE_{dis} value for methanol (−278 kJ mol^{-1}) was much less negative than those for the larger alcohols (e.g., −334 kJ mol^{-1} for 2-butanol), consistent with stronger van der Waals interaction between the latter and solid surfaces. This difference in ΔE_{dis} suggests that the solvent-occupied active sites on α-MoC surfaces can be accessed by furfural reactants more easily in methanol than in 2-butanol, which benefits furfural hydrogenation rates. However, the hydrogen donating ability of methanol is weaker than that for 2-butanol,[48] and the smaller size of methanol leads to more crowded lateral

DOI: 10.1021/jacs.8b09310
J. Am. Chem. Soc. XXXX, XXX, XXX−XXX

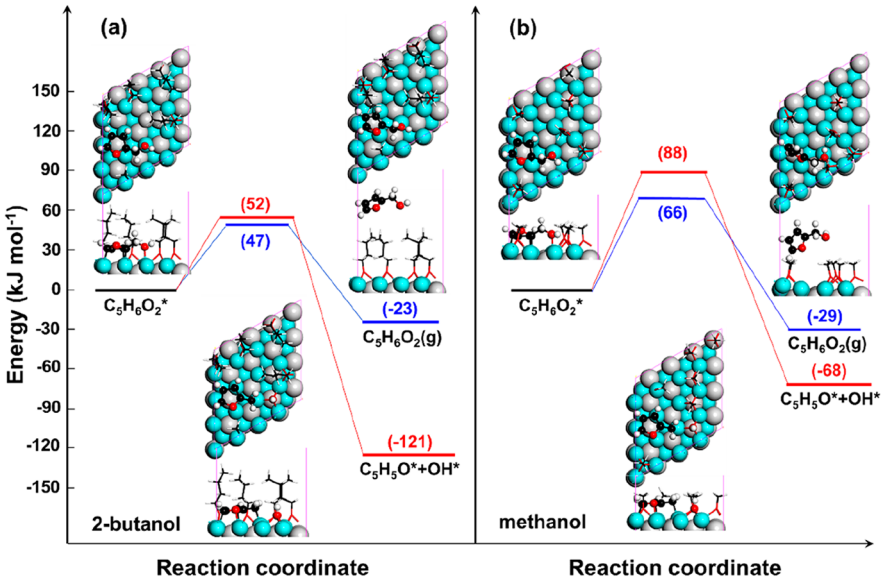

Figure 4. Energy profiles for hydrogenolysis (red line) and desorption (blue line) of adsorbed furfuryl alcohol on α-MoC(111) surfaces covered with (a) four butoxide species derived from 2-butanol dissociative adsorption and (b) six methoxide species derived from methanol dissociative adsorption. For the energy of gaseous furfuryl alcohol, the entropy correction at 423 K has been included. In top and side view of the corresponding optimized structures, Mo, C, O, and H atoms are given in cyan, gray, red, and white, respectively. The C atoms in the organic species are, however, in dark for making a distinction from those in the α-MoC layers.

environment for reactions occurred on α-MoC surfaces as shown next in this section, which, in fact, destabilizes kinetically relevant hydrogenation transition states. These two negative effects on the furfural hydrogenation rates compensate for that brought forth by the better accessibility of α-MoC active sites in methanol (with respect to 2-butanol), thus accounting for the similar furfural hydrogenation rates measured in methanol and 2-butanol solvents (Figure 2).

The selectivities to furfuryl alcohol and 2-methyl furan in furfural hydrogenation is determined by relative activation barriers for desorption and hydrogenolysis of furfuryl alcohol species adsorbed on α-MoC, as shown from Scheme 1. These events occur at nearly full surface coverages of the alcohol solvent molecules during catalysis, because of the thermodynamically favored nature of alcohol dissociation on α-MoC (Figure 3) and the low molar ratios of furfuryl alcohol to the solvent molecule (~1/200). Weak interactions between surface species and free solvent molecules above the dissociatively adsorbed solvent layer are not taken into account in the DFT treatments of these branching surface events, because the effects of free solvent molecules on the relative activation barriers of these events are mostly canceled out as a result of the similar sizes of the involved transition states.

When 2-butanol is chosen as the solvent, each adsorbed furfuryl alcohol (at a surface density of 0.39 molecules nm^{-2}) can be surrounded by four alkoxides formed from 2-butanol dissociation to reach surface saturation. The calculated activation barrier for furfuryl alcohol desorption at such crowded α-MoC surfaces is 47 kJ mol^{-1} (Figure 4a; DFT-optimized transition state (TS) structure in Figure S17), similar to the corresponding activation barrier for furfuryl alcohol hydrogenolysis via the kinetically relevant cleavage of the C−O bond (52 kJ mol^{-1}, Figure 4a; DFT-optimized TS structure in Figure S15). When methanol, smaller than 2-butanol in size, is chosen as the solvent, the maximum number of alkoxide species surrounding each adsorbed furfuryl alcohol increases to six (2.3 molecules nm^{-2}), which makes the α-MoC surface more crowded than the case for 2-butanol solvents. The calculated activation barriers for desorption and hydrogenolysis of furfuryl alcohol at these methoxide-modified α-MoC surfaces are 66 and 88 kJ mol^{-1} (Figure 4b; DFT-optimized TS structures in Figure S17), respectively, consistent with the increase of steric hindrance for forming the involved transition states as the solvent changes from 2-buranol to methanol.

The activation barrier for the hydrogenolysis reaction increases with the steric hindrance more sensitively than for the desorption process (36 vs 19 kJ mol^{-1} for replacing the 2-buranol solvent by methanol, Figure 4), reflecting the hydrogenolysis transition states that involve more active sites because of the requirement for stabilizing the OH group incipiently separated from furfuryl alcohol at these hydrogenolysis transition states (Figure S17). This difference of the activation barrier dependence on the size of the solvent molecule leads to a strong inhibition of the 2-methyl furan formation when the solvent is methanol, which agrees well with those low 2-methyl furan selectivities in methanol as observed from experiments (Figures 2 and S14).

In summary, the above theoretical treatments suggest that the α-MoC catalysts are highly covered by the alcohol solvents at reaction conditions, thus making the activity and selectivity of furfural hydrogenation on such alcohol-modified surfaces controllable via the size of the alcohol solvent molecules.

3.4. Effects of H_2O on Activity and Selectivity of Furfural Hydrogenation Reactions on α-MoC Catalysts.

Pure H_2O solvent is not adaptable for practical furfural conversions, because of the low solubility of furfural in H_2O (83 g L^{-1} at 298 K). H_2O is, however, an inevitable product formed from furfural hydrogenation to 2-methyl furan (Scheme 1), and the furfural feedstock is commercially produced via acid-catalyzed hydrolysis and dehydration of xylan in aqueous media. Therefore, it is crucial to assess the

DOI: 10.1021/jacs.8b09310
J. Am. Chem. Soc. XXXX, XXX, XXX−XXX

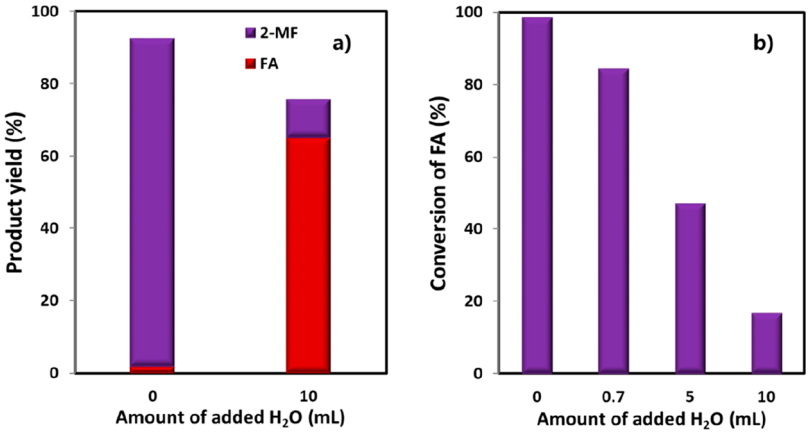

Figure 5. Effects of added H_2O on (a) product yields of furfural hydrogenation and (b) conversions of furfuryl alcohol on α-MoC catalysts (423 K, 2.0 MPa H_2, 1 mL furfural, 50 mL solvent, 150 mg α-MoC, 6 h; FA for furfuryl alcohol, 2-MF for 2-methyl furan).

effects of H_2O on the rate and selectivity of furfural hydrogenation on α-MoC.

Figure 5a depicts that the addition of H_2O (10 mL) into the 2-butanol solvent (40 mL) led to a slight decrease of the yield of furfural hydrogenation products (i.e., the sum for 2-methyl furan and furfuryl alcohol) from 92.4% to 75.6% (423 K, 2 MPa H_2, 150 mg α-MoC). In contrast, the selectivity to 2-methyl furan decreased sharply as H_2O was introduced (e.g., 93.6% for pure 2-butanol, 10.6% for 10 mL added H_2O, Figure 5a). Similar effects of H_2O addition on the furfural hydrogenation rate and selectivity were also found when the solvent was 2-propanol (Figure S18, SI). This general trend reflects that the presence of H_2O restrains the hydrogenolysis of the primary furfuryl alcohol product to 2-methyl furan, further evidenced by a monotonic decrease of the hydrogenolysis rate of furfuryl alcohol (with ~100% selectivity to 2-methyl furan) as H_2O is gradually added to the alcohol solvent (Figure 5b). This significant effect of H_2O addition on the furfural hydrogenation selectivity is reminiscent of that for methanol (Figure 2), indicating H_2O makes the hydrogenolysis of adsorbed furfuryl alcohol on α-MoC kinetically less favored with respect to its desorption into liquid phase, brought forth by more crowded α-MoC surfaces in the presence of small H_2O solvent molecules during catalysis.

4. CONCLUSIONS

Pure-phase molybdenum carbides (α-MoC, β-Mo_2C) and nitrides (γ-Mo_2N) efficiently catalyze liquid-phase hydrogenation of furfural to furfuryl alcohol and 2-methyl furan with high selectivity, among which α-MoC exhibits the most active surfaces. Furfural hydrogenation rates and selectivities on these Mo-based catalysts can be further mediated by using alcohols as solvent. On one hand, primary and secondary alcohols act as hydrogen donors to promote hydrogenation rates. On the other hand, the thermodynamically favored dissociative adsorption of alcohols on these molybdenum carbides (and nitrides) leads to highly covered catalytic surfaces at reaction conditions, rendering the accessibility of active sites and the steric hindrance for forming reaction transition states on catalytic surfaces tunable by the size of alcohol, as also observed for H_2O that is formed in situ or added before reaction. Combination of these solvent effects results in high yields (>90%) of furfuryl alcohol in methanol solvent and of 2-methyl furan in 2-butanol solvent on α-MoC with similar furfural conversion rates. The preferential activation of C═O and C−OH bonds over C═C and C−C bonds on molybdenum carbides (and nitrides) and the controllable hydrodeoxygenation rates and selectivities on these catalysts conferred by the solvent-induced surface modification are expected to shed light on new catalytic materials and reaction processes for efficient biomass upgrading at mild conditions.

■ ASSOCIATED CONTENT

Supporting Information

The Supporting Information is available free of charge on the ACS Publications website at DOI: 10.1021/jacs.8b09310.

Catalyst characterization by XRD, TEM, XPS, and XAFS; effects of stirring speed, H_2O addition, and reaction atmosphere (H_2, D_2, and N_2) on furfural hydrogenation rates; conversion-selectivity profiles of furfural hydrogenation; catalyst recycle performance; reactivity comparison between furfural and furfuryl alcohol; MoC surface structures; DFT-derived structures of adsorbed alcohols on MoC and their dissociative adsorption energy as a function of surface coverage; and DFT-derived transition states for furfuryl alcohol desorption and hydrogenolysis on MoC (PDF)

■ AUTHOR INFORMATION

Corresponding Authors

*shuaiwang@xmu.edu.cn

*dma@pku.edu.cn

ORCID

Xiao-Dong Wen: 0000-0001-5626-8581

Ding Ma: 0000-0002-3341-2998

Author Contributions

#These authors contributed equally to this work.

Notes

The authors declare no competing financial interest.

■ ACKNOWLEDGMENTS

This work was financially supported by the National Key R&D Program of China (2017YFB0602200) and Natural Science Foundation of China (21725301, 91645115, 21473003, and 21821004). XAFS experiments were performed at Shanghai

DOI: 10.1021/jacs.8b09310
J. Am. Chem. Soc. XXXX, XXX, XXX−XXX

Synchrotron Radiation Facility (SSRF) and 1W1B beamline of Beijing Synchrotron Radiation Facility (BSRF).

REFERENCES

(1) Mamman, A. S.; Lee, J. M.; Kim, Y. C.; Hwang, I. T.; Park, N. J.; Hwang, Y. K.; Chang, J. S.; Hwang, J. S. *Biofuels, Bioprod. Biorefin.* **2008**, *2*, 438−454.
(2) Aldosari, O. F.; Iqbal, S.; Miedziak, P. J.; Brett, G. L.; Jones, D. R.; Liu, X.; Edwards, J. K.; Morgan, D. J.; Knight, D. K.; Hutchings, G. J. *Catal. Sci. Technol.* **2016**, *6*, 234−242.
(3) Ma, X.; Jiang, C.; Xu, H.; Ding, H.; Shuai, S. *Fuel* **2014**, *116*, 281−291.
(4) Li, J.; Liu, J.-l.; Zhou, H.-J.; Fu, Y. *ChemSusChem* **2016**, *9*, 1339−1347.
(5) Mariscal, R.; Maireles-Torres, P.; Ojeda, M.; Sadaba, I.; Lopez Granados, M. *Energy Environ. Sci.* **2016**, *9*, 1144−1189.
(6) Dong, F.; Ding, G.; Zheng, H.; Xiang, X.; Chen, L.; Zhu, Y.; Li, Y. *Catal. Sci. Technol.* **2016**, *6*, 767−779.
(7) Pang, S. H.; Medlin, J. W. *ACS Catal.* **2011**, *1*, 1272−1283.
(8) Pang, S. H.; Schoenbaum, C. A.; Schwartz, D. K.; Medlin, J. W. *ACS Catal.* **2014**, *4*, 3123−3131.
(9) Wang, C.; Wang, L.; Zhang, J.; Wang, H.; Lewis, J. P.; Xiao, F.-S. *J. Am. Chem. Soc.* **2016**, *138*, 7880−7883.
(10) Maligal-Ganesh, R. V.; Xiao, C.; Goh, T. W.; Wang, L.-L.; Gustafson, J.; Pei, Y.; Qi, Z.; Johnson, D. D.; Zhang, S.; Tao, F.; Huang, W. *ACS Catal.* **2016**, *6*, 1754−1763.
(11) Taylor, M. J.; Jiang, L.; Reichert, J.; Papageorgiou, A. C.; Beaumont, S. K.; Wilson, K.; Lee, A. F.; Barth, J. V.; Kyriakou, G. *J. Phys. Chem. C* **2017**, *121*, 8490−8497.
(12) Wang, C.; Guo, Z.; Yang, Y.; Chang, J.; Borgna, A. *Ind. Eng. Chem. Res.* **2014**, *53*, 11284−11291.
(13) Liu, X.; Zhang, B.; Fei, B.; Chen, X.; Zhang, J.; Mu, X. *Faraday Discuss.* **2017**, *202*, 79−98.
(14) Zhang, Z.; Song, J.; Jiang, Z.; Meng, Q.; Zhang, P.; Han, B. *ChemCatChem* **2017**, *9*, 2448−2452.
(15) Panagiotopoulou, P.; Martin, N.; Vlachos, D. G. *ChemSusChem* **2015**, *8*, 2046−54.
(16) Panagiotopoulou, P.; Martin, N.; Vlachos, D. G. *J. Mol. Catal. A: Chem.* **2014**, *392*, 223−228.
(17) Fang, R.; Liu, H.; Luque, R.; Li, Y. *Green Chem.* **2015**, *17*, 4183−4188.
(18) Dong, F.; Zhu, Y.; Zheng, H.; Zhu, Y.; Li, X.; Li, Y. *J. Mol. Catal. A: Chem.* **2015**, *398*, 140−148.
(19) Jiménez-Gómez, C. P.; Cecilia, J. A.; Moreno-Tost, R.; Maireles-Torres, P. *Top. Catal.* **2017**, *60*, 1040−1053.
(20) Pang, S. H.; Love, N. E.; Medlin, J. W. *J. Phys. Chem. Lett.* **2014**, *5*, 4110−4114.
(21) Shi, Y.; Zhu, Y.; Yang, Y.; Li, Y.-W.; Jiao, H. *ACS Catal.* **2015**, *5*, 4020−4032.
(22) Yang, P.; Xia, Q.; Liu, X.; Wang, Y. *Fuel* **2017**, *187*, 159−166.
(23) Zhou, M.; Li, J.; Wang, K.; Xia, H.; Xu, J.; Jiang, J. *Fuel* **2017**, *202*, 1−11.
(24) An, W.; Men, Y.; Wang, J. *Appl. Surf. Sci.* **2017**, *394*, 333−339.
(25) Audemar, M.; Ciotonea, C.; De Oliveira Vigier, K.; Royer, S.; Ungureanu, A.; Dragoi, B.; Dumitriu, E.; Jerome, F. *ChemSusChem* **2015**, *8*, 1885−1891.
(26) McManus, J. R.; Vohs, J. M. *Surf. Sci.* **2014**, *630*, 16−21.
(27) Xiong, K.; Lee, W. S.; Bhan, A.; Chen, J. G. *ChemSusChem* **2014**, *7*, 2146−2149.
(28) Farrell, W. M. *Chem* **2018**, *4*, 12−14.
(29) Gong, W.; Chen, C.; Zhang, Y.; Zhou, H.; Wang, H.; Zhang, H.; Zhang, Y.; Wang, G.; Zhao, H. *ACS Sustainable Chem. Eng.* **2017**, *5*, 2172−2180.
(30) Chen, J. G. *Chem. Rev.* **1996**, *96*, 1477−1498.
(31) Lin, L.; Zhou, W.; Gao, R.; Yao, S.; Zhang, X.; Xu, W.; Zheng, S.; Jiang, Z.; Yu, Q.; Li, Y. W.; Shi, C.; Wen, X. D.; Ma, D. *Nature* **2017**, *544*, 80−83.
(32) Hwu, H. H.; Chen, J. G. *Chem. Rev.* **2005**, *105*, 185−212.
(33) Gilkey, M. J.; Panagiotopoulou, P.; Mironenko, A. V.; Jenness, G. R.; Vlachos, D. G.; Xu, B. *ACS Catal.* **2015**, *5*, 3988−3994.
(34) Lee, W.-S.; Wang, Z.; Zheng, W.; Vlachos, D. G.; Bhan, A. *Catal. Sci. Technol.* **2014**, *4*, 2340−2352.
(35) Yao, S.; Zhang, X.; Zhou, W.; Gao, R.; Xu, W.; Ye, Y.; Lin, L.; Wen, X.; Liu, P.; Chen, B.; Crumlin, E.; Guo, J.; Zuo, Z.; Li, W.; Xie, J.; Lu, L.; Kiely, C. J.; Gu, L.; Shi, C.; Rodriguez, J. A.; Ma, D. *Science* **2017**, *357*, 389−393.
(36) Bertero, N. M.; Trasarti, A. F.; Apesteguía, C. R.; Marchi, A. J. *Appl. Catal., A* **2011**, *394*, 228−238.
(37) Ravel, B.; Newville, M. *J. Synchrotron Radiat.* **2005**, *12*, 537−541.
(38) Kresse, G.; Furthmüller, J. *Comput. Mater. Sci.* **1996**, *6*, 15−50.
(39) Kresse, G.; Furthmüller, J. *Phys. Rev. B: Condens. Matter Mater. Phys.* **1996**, *54*, 11169−11186.
(40) Blöchl, P. E. *Phys. Rev. B: Condens. Matter Mater. Phys.* **1994**, *50*, 17953−17979.
(41) Kresse, G.; Joubert, D. *Phys. Rev. B: Condens. Matter Mater. Phys.* **1999**, *59*, 1758−1775.
(42) Perdew, J. P.; Burke, K.; Ernzerhof, M. *Phys. Rev. Lett.* **1996**, *77*, 3865−3868.
(43) Methfessel, M.; Paxton, A. T. *Phys. Rev. B: Condens. Matter Mater. Phys.* **1989**, *40*, 3616−3621.
(44) Grimme, S.; Ehrlich, S.; Goerigk, L. *J. Comput. Chem.* **2011**, *32*, 1456−1465.
(45) Henkelman, G.; Uberuaga, B. P.; Jónsson, H. *J. Chem. Phys.* **2000**, *113*, 9901−9904.
(46) Monkhorst, H. J.; Pack, J. D. *Phys. Rev. B: Condens. Matter Mater. Phys.* **1976**, *13*, 5188−5192.
(47) Lin, Z.; Chen, R.; Qu, Z.; Chen, J. G. *Green Chem.* **2018**, *20*, 2679−2696.
(48) Gilkey, M. J.; Xu, B. *ACS Catal.* **2016**, *6*, 1420−1436.

DOI: 10.1021/jacs.8b09310
J. Am. Chem. Soc. XXXX, XXX, XXX−XXX